Induction and Conduction Thermography: From the Basics to Application

Johannes VRANA [1], Matthias GOLDAMMER [2]
[1] Vrana GmbH - NDE Consulting & Solutions, Rimsting
[2] Siemens AG Corporate Technology, Munich
Contact e-mail: dgzfp@vrana.net

Abstract. Active thermography, using electromagnetic excitation, is a non-contacting, non-destructive evaluation method with a wide range of applications. It allows detecting inhomogenities, like cracks, at or close to the surface of metallic components fast and reliable utilizing infrared imaging.
Electric current can be used in two ways for thermography: In induction thermography a current is coupled to the component by passing an AC current through a coil which is in close proximity to the component inspected, while in conduction thermography the current is coupled directly into the component.
In this paper, we present the basics of this NDE method, along with several component examples and how to build systems for the inspection. The detectability of cracks with high residual stresses will be discussed and compared to other surface testing methods as well as the reliability of the method and the prospects for automation.

Introduction

A component can be excited in a thermographic inspection in one of two electromagnetic ways, either inductively or conductively [1, 2, 3, 4, 5].

Induction thermography has been in use since the late 70s to test steel bars in roll mills for cracks [6]. Due to the advances in infrared camera and generator technology this non-destructive testing method has gained more and more interest and has been examined by many groups worldwide [7, 8, 9, 10, 11, 12].

As illustrated in Fig. 1, inductive excitation is achieved by an alternating current (AC) running through an inductor placed next to the sample, and conductive excitation is achieved by direct galvanic contacts. In this case an excitation with an alternating (AC) or direct current (DC) is possible. With both methods, a current is created in the electrically conducting material and depending on the current density, heating occurs in the sample. If a crack is present, the current is disrupted, resulting in an alternated current density distribution around the cracked area. Therefore, when the heat diffuses to the surface, the crack can be detected with an infrared camera. This process of thermographic crack detection using electromagnetic excitation is discussed in [1, 3] in detail.

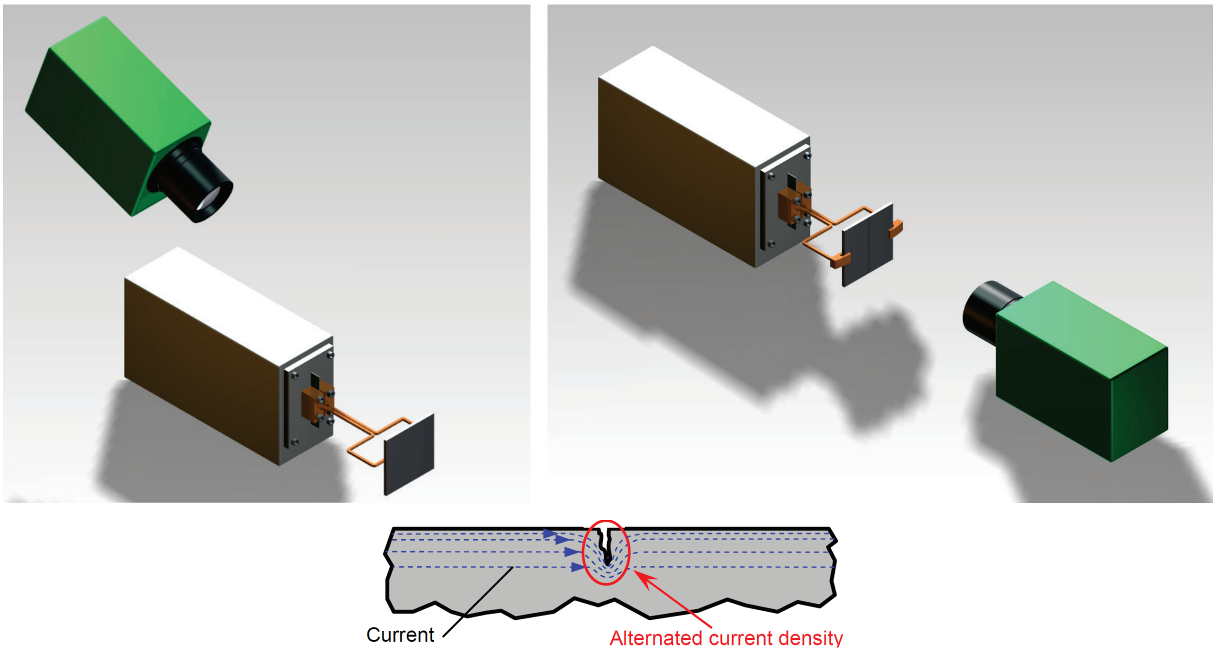

Fig. 1: Top left: Typical induction thermography measurement set-up.
Top right: Typical conduction thermography measurement set-up.
Cracks or other inhomogeneities lead to alternated current density distributions (bottom) [2].

During inductive excitation, the current density is highest directly under the inductor (distribution at the surface is described by the proximity effect and in the depth of the material by the skin effect) and the current flows back in the edges of the front and back surface [1, 3]. With DC conductive excitation, the current density is homogeneously distributed if no defects are present. With AC excitation, the current density is highest at the four edges of the conductor and decreases in between. This is called the edge effect. Additionally, the skin effect is present as the current density rises from the middle to the sides [3].

When building inspection systems, it is important to identify the appropriate parameters. Factors such as the material under test, the type of induction generator, the type of infrared camera, and the signal processing are critical for a successful system development.

1. Optimizing the Inspection System

1.1 Heating

Starting with the excitation, the result of the inspection depends on the inductive or galvanic coupling of the current into the sample, the current density distribution created in the sample, and the temperature distribution due to the heat diffusion. So, to optimize the inspection system all those parameters must be maximized to improve the signal-to-noise ratio (SNR) resulting in an image with highest possible contrast.

The SNR depends on the heating of the sample Q which depends on the power in the part P and on the time span τ of the excitation:

$$Q = P \cdot \tau. \tag{1}$$

Therefore, to optimize the SNR the power should be maximized and as the power is quadratically dependent [2, 3] on the current flowing through the part or respectively on the current flowing through the inductor the generator chosen for the inspection should be optimized for high currents. By using standard generators available on the current market (500 - 2000A) most electrically conductive materials can be tested. Moreover, even low electrically conductive materials are inspectable. To the contrary, due to the limited maximum current materials with higher electric conductivity (like Aluminum and Copper) require a more sophisticated method of inspection and signal processing. Furthermore, materials with a high permeability (due to the skin effect and the increased power) are especially suited for surface crack detection using thermography. It is important that the current and frequency of the AC current must be adapted to the permeability of the material.

Moreover, as (1) reveals the time duration of the excitation is a second factor to optimize the SNR. However, the thermal diffusion process leads to blurring of the image over time (especially of small heat sources as created by cracks). Utilizing the thermal diffusivity α the thermal penetration depth for a pulsed excitation is:

$$d_{th} = 2\sqrt{\alpha t}. \tag{2}$$

As the power of the generator is limited, a compromise is necessary to get enough heat into the sample and get a sharp result image at the same time. This compromise is quite easy for most materials and results in excitation times of about 50 - 200 ms. Only materials with a high diffusivity require a fast camera and a more sophisticated method of inspection. This is especially the case if a high diffusivity is combined with a high electrical conductivity, normally the case for most metals as thermal and electrical conductivity go hand in hand.

Therefore, for a multi-purpose system the generator should provide the ability to provide a current of about 500 - 2000 A, pulse durations of about 5 - 2000 ms, and the infrared camera should have a low noise equivalent temperature difference (NETD) with enough speed to capture even relatively fast thermal processes (starting from 100 Hz).

1.2 Signal Processing

Besides optimizing the excitation, the resulting images should be optimized to compress all the information available into a single picture showing only the indications. Moreover, for automatic data processing component shape signals must be differentiated from indication signals.

Fig. 2 presents a view of the background subtracted infrared sequence [3] which reveals the indication clearly. Also, some blurring of the signal with time (the blurring is especially visible at the crack: after 260 ms the crack signal is quite blurred and after 597 ms the crack is hardly visible), the heat distribution next to the inductor, and the heating of edges and corners can be seen.

Post-processing the image sequence will help to reduce those artefacts. A pulse-phase analysis [13] of the sequence, containing the heating and cooling phase, will split the information contained in the sequence into two pictures. One of the pictures contains the amplitude-based information and one the time-based (phase) information. As the phase image reveals the crack and suppresses the differences in the emissivity of the part and some of the non-uniformities of the heating (Fig. 2 bottom) this is the image to be used.

A comparison with the result of the dye-penetrant inspection shows that the extent of the indication shown by induction thermography is larger compared to the results of the dye-penetrant inspection. Moreover, the section of the indication not visible in the PT result shows a different heating pattern in the thermographic result. This effect will be discussed in more detail in chapter 4 of this paper.

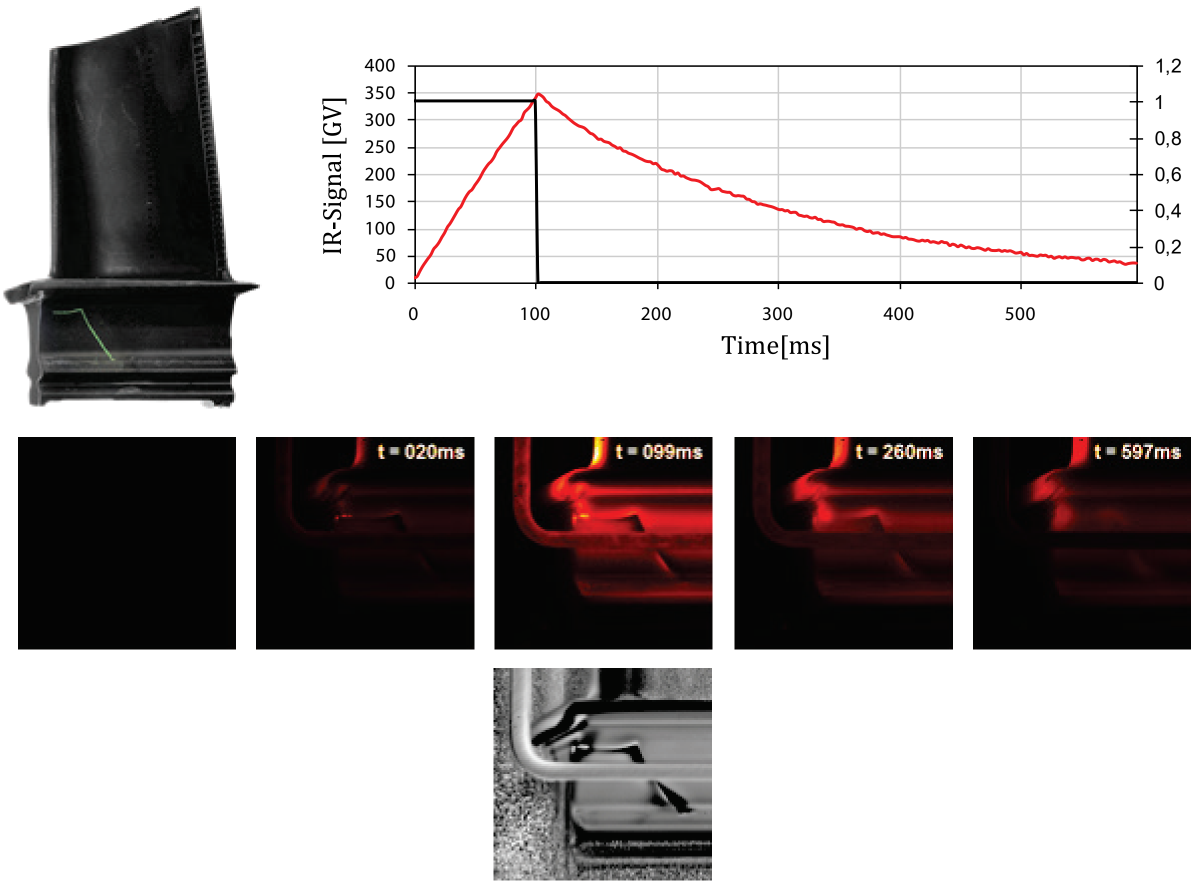

Fig. 2: Top left: Turbine blade to be inspected showing the result of a dye-penetrant inspection for comparison;
Top right: Typical infrared signal of an active thermography inspection with a 100 ms long excitation at a selected position;
Top sequence: Background subtracted infrared images with images at 0, 20, 99, 260, and 597 ms;
Bottom: Pulse-Phase-Analysis of the infrared sequence shortened to 100 ms excitation time and 100 ms cool down time (total observation time is therefore 200 ms) [2].

A very similar result to the pulse-phase analysis can be obtained with a lock-in analysis. For the lock-in analysis, a periodical excitation is necessary and also results in a phase and an amplitude picture. Therefore, the pulse-phase analysis is more or less a lock-in analysis using only a single cycle. However, as it is shown in this paper, when using only one cycle the heating will be insufficient for materials with a high electric conductivity and diffusivity (in some cases). However, by using the lock-in approach, a short excitation time can be used and the necessary heating of the part can be accumulated by using a sufficient number of cycles.

However, even by using pulse-phase or lock-in, an automatic image processing is still hard to accomplish as the resulting picture still shows the component geometry and some other effects. This can be resolved by automated production testing. In this case a standard non-flawed component can be used as a reference. Fig. 3 shows this in more detail. By subtracting the image of the standard component from the component under test only the real indication remains visible. This result can be even improved by combining it with pulse-phase or lock-in [3]. Only some small artifacts due to positioning or size problems remain, but the signal vs. background is clear enough to enable automatic image processing.

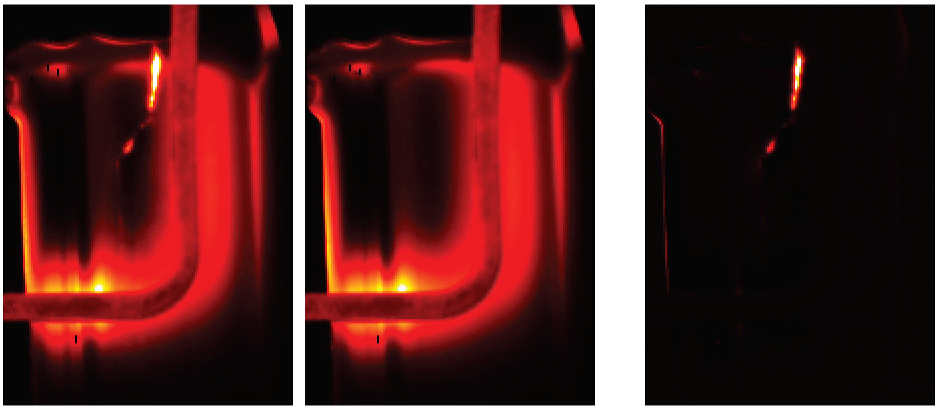

Fig. 3: From left to right: Component under test, standard non-flawed component, resulting image [2].

2. Thermography Systems

2.1 Induction Thermography Systems

Fig. 4 shows a typical lab induction thermography system. This system is based on a 10 kW induction generator which is completely computer controlled. The minimal possible pulse length is 5 ms and the system can be adapted to different materials due to exchangeable condensers. Moreover, the relative position between inductor and part can be adjusted by motors and a lock-in measurement can be done by switching the current of the generator on and off. However, the auxiliary device is connected with the generator by a 2 m long, 5 cm thick and quite stiff cable. Therefore, this is a stationary multi-purpose system capable of inspecting nearly every material. In some cases it is necessary to inspect parts at field locations. For those cases, a mobile and handheld system capable of producing a high current was developed. This system provides arbitrary positioning and immediate access for the interpretation of the measurement to identify and mark cracks.

Fig. 4: Left: Stationary lab induction thermography system
(top: infrared camera, right: auxiliary device of the induction generator);
Right: Mobile and handheld induction thermography system
(left: portable rack including the generator and all the necessary equipment, right: auxiliary device with a small infrared camera and a touch screen display mounted to it) [2].

This can be achieved by using a different standard induction generation with 10 kW. The auxiliary device is included at the end of the more flexible and longer (5 m) cable. Therefore, the inductor can be positioned arbitrarily within the radius of the cable. The capacitors of the induction generator are not exchangeable, but the generator is optimized for material with a low permeability (non-ferromagnetic materials), which results in a maximum usable current of approximately 980 A. Moreover, this type of control is much easier and the induction pulse can by modulated up to a frequency of 300 Hz for lock-in measurements (instead of only switching the generator on and off).

To optimize the design of a portable system, it was integrated into a 19” case (Fig 4). It includes the induction generator, a computer for controlling the system, a keyboard and a display. The connection between computer and all periphery equipment is accomplished via a connector box developed for this purpose. The excitation and the post processing are integrated in the software.

More flexibility of the system is possible by mounting some additional equipment on the auxiliary device. By activating a button to start the measurement, a small infrared camera captures the image displayed on a small screen. This system can be applied at the part location, exciting the component and interpreting the resulting image displayed after the measurement on the small screen. The uncooled camera lacks the resolution of cooled detector butis sufficient for many inspection cases as the resulting image in the display in Fig 4 reveals. By using a touch screen display the system can be operated remotely, for example by using the touch-screen to mark and evaluate the indications.


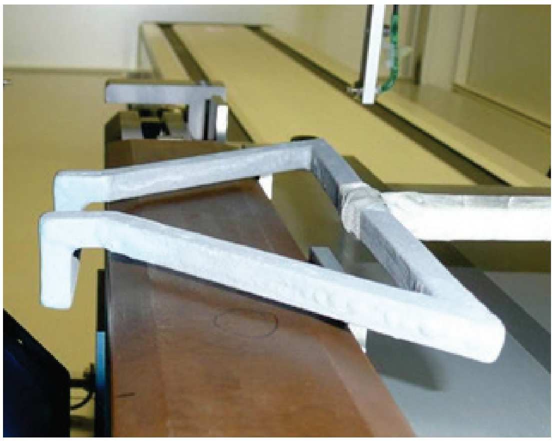

Fig. 5: Left: View of the automated induction thermography inspection system from the outside
Right: Component under test and induction coil [4].

Induction thermography is also suited for automated inspections. Fig. 5 shows an example of an inspection system [4]: Situated on the left-hand side is the loading area where steel bars are inserted before the inspection and removed afterwards. The part on the right-hand side contains the induction coil and the infrared camera above the coil, shielding the component during the inspection from the infrared radiation of the surroundings and the inspector. Once inserted the component is moved automatically from the loading bay into the inspection area and is therefore moved past the exciting coil and recording camera. The operator controls the system via computer from the display and keyboard mounted on a swivel arm.

In order to detect cracks independently of their orientation the current has to be induced in two directions perpendicular to each other. In this system, the two sides of a triangular coil are used which form an angle of 90° to each other (Fig. 5).

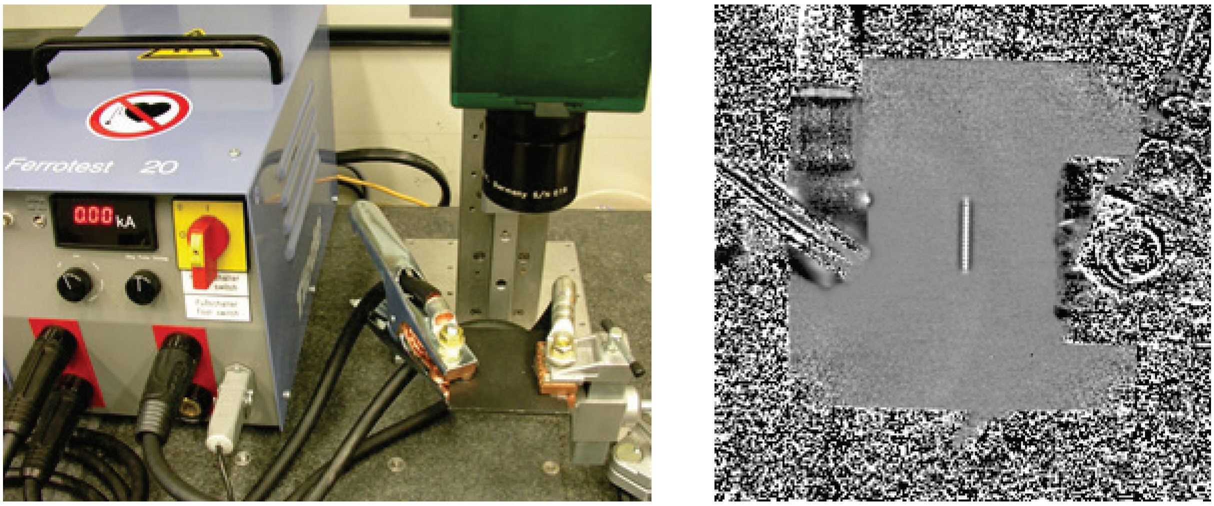

Fig. 6: Conduction thermography system and resulting image calculated by pulse-phase analysis. analysis. The “crack” (several holes drilled into the component next to each other) in the center of the test component is clearly visible [2].

2.2 Conduction Thermography Systems

Besides the induction thermography systems, conduction thermography system using direct contact were tested. Fixing the part allows the use of pulse-phase and lock-in analysis. Therefore, the part in Fig 6 is clamped on one side. This fixture is also the first electrical contact. The other electrical contact is the clamp on the left side. The maximum current produced by the generator is 2000 A and is sufficient for most parts to be inspected with a reasonable excitation time.

With this system, a sample was inspected containing some drilled holes. The resulting image (Fig. 6 right) was gained with the pulse-phase analysis suppressing artifacts and showing the indication clearly. The low noise level indicates that nearly the whole part was inspected for indications.

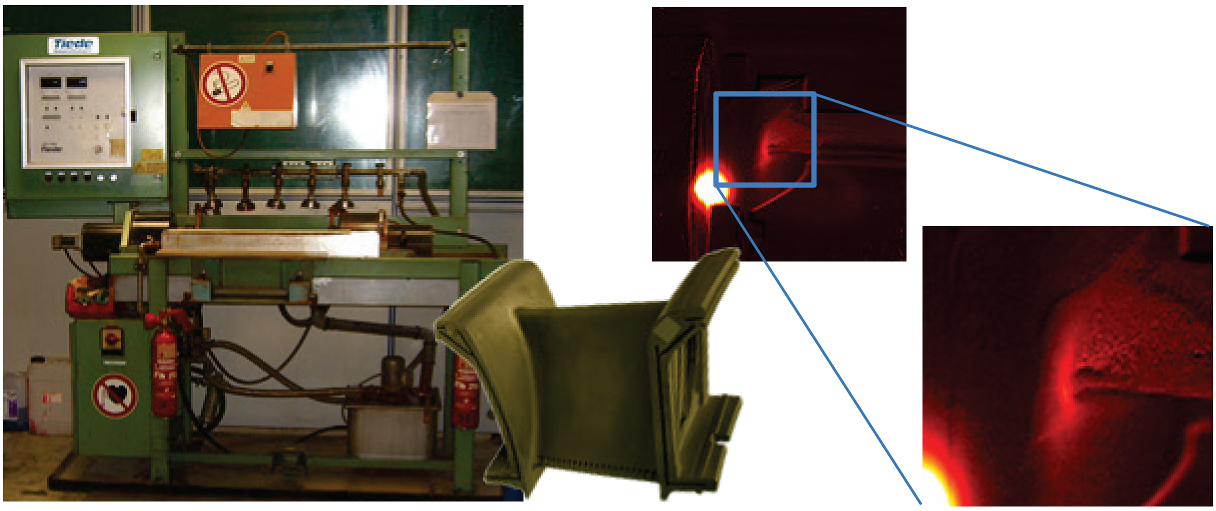

Fig. 7: Conduction thermography system and resulting image calculated by pulse-phase analysis [2].

To bring this one step closer to an application a magnetic particle inspection system (Horizontal Wet Unit) was used for the excitation by direct contact and instead of the magnetic particles an infrared camera is used for detection. As Fig. 7 shows a subsurface crack in a gas turbine vane with a low permeable non-ferromagnetic material is clearly indicated. Only a heat-spot due to the contacting of the part is visible which can be eliminated by adapting the fixturing to the part under test. Therefore, magnetic particle inspection stations, slightly modified, can be used to inspect ferromagnetic and non-ferromagnetic parts for cracks by replacing the magnetic particles with an infrared camera.

3. Crack Detection Mechanisms and Models

3.1 Open Cracks

A crack can be described by its specific length and its depth profile. Therefore, depending on the nature of the crack the current flows either around the crack tips or beneath the crack. To model this behavior, it is therefore best to look at these two alternatives individually.

A model for the case where the current has to flow around the crack tip is given by a slot which is finite in length but extends completely through the sample (see Fig. 8). In this case the current density is highest at the crack tips and lowest besides the crack. Therefore, the typical thermographic signal for such a crack is characterized by the hot-spots at the crack tips and a colder zone at the sides of the crack.

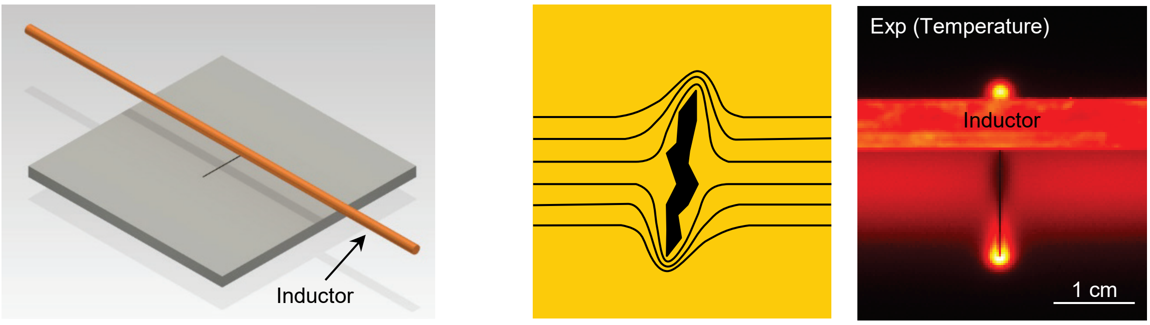

Fig. 8: Model and typical thermographic result of a slot-like crack [1].

For the second case, we use a notch infinite in length but finite in depth as model geometry (see Fig. 9). In this case the current has to flow beneath the crack and therefore the current density is highest at the bottom of the notch and lowest at the top edges. However, the heat from the bottom is diffusing to the surface and therefore after the induction pulse is finished the top edges tend to stay warmer than the surrounding material.

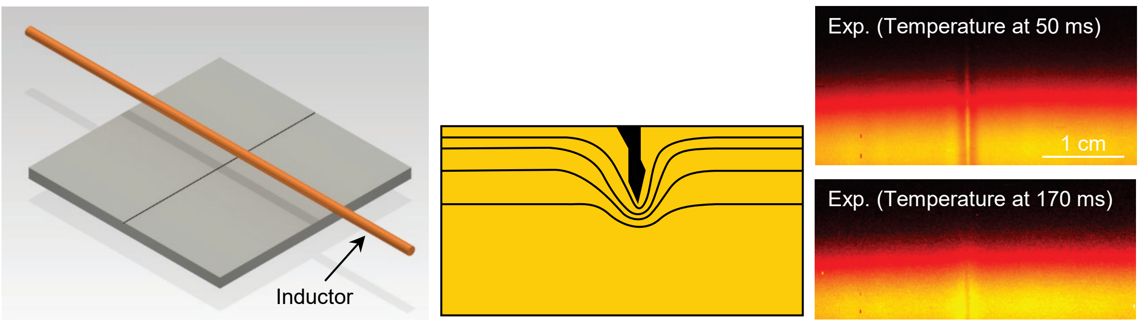

Fig. 9: Model and typical thermographic result of a notch-like crack (50 ms induction pulse) [1].

3.1 Closed Cracks

The slot and the notch already give a good model for the induction heating effects related to cracks, but looking at a real crack, as shown in Fig. 10, it becomes clear that additional heating mechanisms have to be examined and the modelling has to be modified for closed cracks.

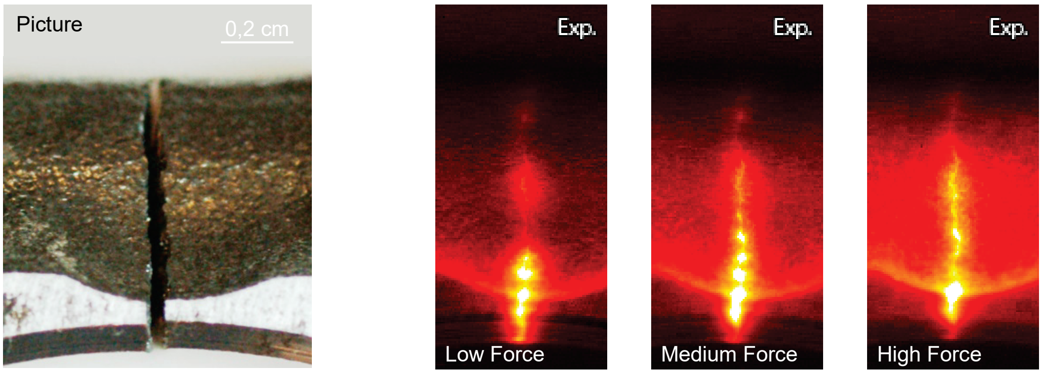

Fig. 10: Result of an induction thermography inspection of a crack closed by nut and bolt (clamping torque: 1, 2, and 10 Nm) [1].

As can be seen this crack shows a hot line along the crack with several hot spots. To model this phenomenon a sample with several adjacent drilled holes was prepared. An experiment with induction thermography shows that every material bridge between the holes leads to a hot spot (see Fig. 11).

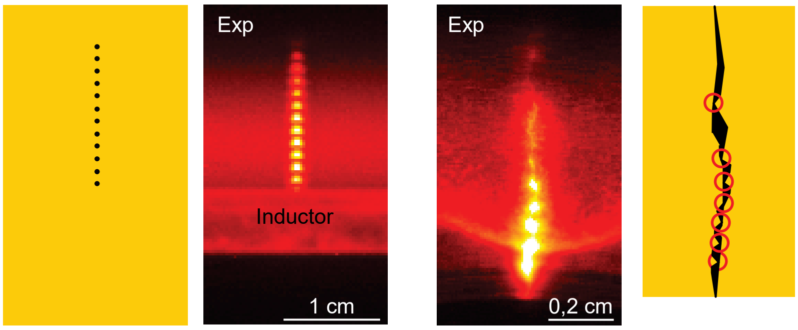

Fig. 11: Left: Indication of holes drilled in a sample; Right: Indication of the crack shown in Fig. 10 and an schematic explanation for the infrared signal (red circles in the figure on the right) [1].

An increase in the density of the contact bridges leads to a situation where the image of the spot distribution gets more and more homogeneous and finally looks like a line. This effect can be seen in Fig. 10. By increasing the clamping force per area the density of the contacting points increases and hence the resulting infrared image of the crack looks more homogeneous.

This contrasts with acoustic thermography [14] or penetrant testing. In acoustic thermography, open cracks give no signal. With increasing residual stresses the signal gets stronger and finally decreases due to the residual stresses supressing the movement of the crack. This means that such cracks produce no heat and will not be detected. An experiment with the same component used in Fig. 10 show that the best signal can be obtained with acoustic thermography with a clamping torque of 5 Nm and that with 10 Nm the signal cannot be distinguished from the noise [14, 15]. Similarly, as it will be shown in chapter 4, it is also very hard (or even impossible) to detect tightly closed cracks with penetrant testing. This makes induction or conduction thermography the ideal techniques once it comes to cracks with high residual stresses.

For cracks with high residual stresses the density of contact points can be higher than what can be resolved by thermography. In that case a crack can alternatively be modelled as a zone of reduced electric conductivity. Fig. 12 shows the result of a simulation of a slot which is filled with a material with a stepwise altered electric conductivity. On the right hand side, the electrical conductivity of the filling material is equal to the surrounding material and the crack leads to no change in the heating. Next, the conductivity was decreased slightly and the crack shows up as a line. By further reducing the conductivity hot spots are showing up at the crack tips and finally only the crack tips can be seen. The latter situation is identical to an open crack.

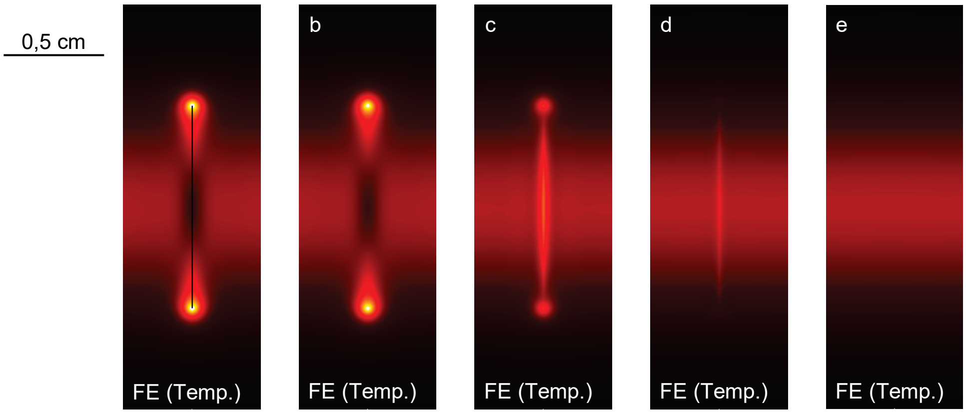

Fig. 12: Images of the temperature distribution calculated by a finite-element simulation for a slot filled with some material with an altered electrical conductivity [1]
a) $\sigma_{Crack} = 0$, b) $\sigma_{Crack} = 1.5\ 10^{-5}\ \sigma_{Material}$, c) $\sigma_{Crack} = 1.4\ 10^{-3}\ \sigma_{Material}$, d) $\sigma_{Crack} = 0.13\ \sigma_{Material}$, e) $\sigma_{Crack} = \sigma_{Material}$.

4. Application Examples

Fig. 13 shows an example of a fatigue crack in a gas turbine blade. The measurement result of the induction thermography inspection has two aspects. Firstly, in the middle figure a large L-shaped indication can be seen which represents an open crack. Secondly, there are some hot spots at the left end of this indication (see enlarged image on the right) which are the result of a closed crack with several contacting points. A dye-penetrant test of this blade has shown that this section of the crack is very difficult to detect as it is tightly closed. This is also why this section of the crack cannot be detected using acoustic thermography [14]. This shows that thermography with electromagnetic excitation should be preferred for components which could have cracks with high residual stresses. For a more detailed discussion see [3].

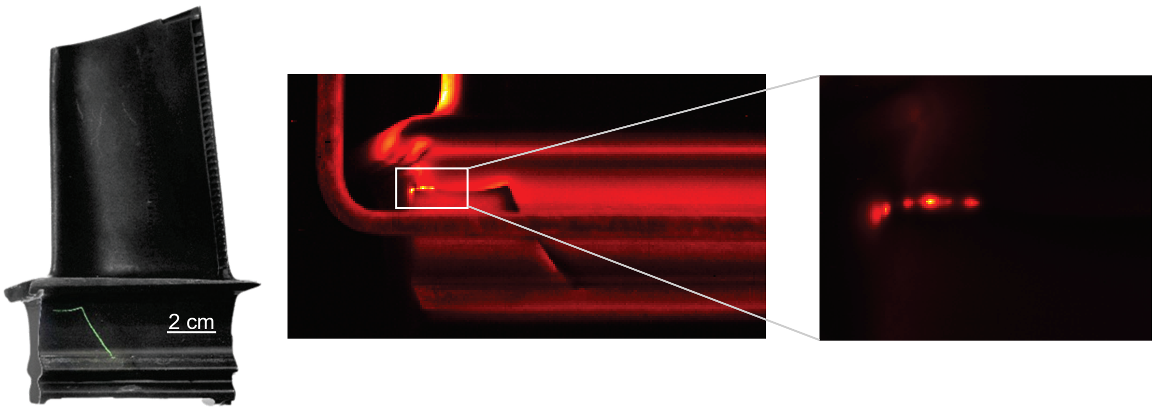

Fig. 12: Dye-penetrant inspection (left picture) compared to an induction thermography inspection of a fatigue crack in the root of a turbine blade (middle and right figure) [1].

5. Summary and Outlook

Active thermography using electromagnetic excitation can be applied by using the inductive and the conductive excitation methods and is ideally suited for detection of cracks close or open to the surface. Typical materials are easy to inspect and using mechanics like robotics, translation or rotary stages automated inspection can be implemented for serial production.

The thermographic technique has the advantage to work contact-free, without coupling media, and without chemicals. UV illumination is not necessary. Image generation is part of the detection process. This allows further post-processing which enables automated indication detection.

The models for crack detection give a good understanding of the thermographic results of real cracks. It also shows that induction and conductions thermography are ideally suited for all kinds of surface or close to the surface cracks, including cracks with high residual stresses which are difficult to detect using acoustic thermography or penetrant testing. This combined with the chances to automate the inspection show the value of thermography with electromagnetic excitation.

Acceptance for the new thermographic techniques will also increase due to new national and European standards on induction thermography, which are being worked out at this time.

References

[1] J. Vrana, M. Goldammer, J. Baumann, M. Rothenfusser, W. Arnold, “Mechanisms and Models for Crack Detection with Induction Thermography”, AIP Conference Proceedings 975, pp. 475-482 (2008)

[2] J. Vrana, M. Goldammer, K. Bailey, M. Rothenfusser, W. Arnold, “Induction and Conduction Thermography: Optimizing the Electromagnetic Excitation Towards Application”, AIP Conference Proceedings 1096, pp. 518-525 (2009)

[3] J. Vrana, “Grundlagen und Anwendungen der aktiven Thermographie mit elektromagnetischer Anregung - Induktions-und Konduktionsthermographie”, Shaker, Herzogenrath (2009)

[4] M. Goldammer, H. Mooshofer, M. Rothenfusser, J. Bass, “Automated Induction Thermography of Generator Components”, AIP Conference Proceedings 1211, pp. 451-457 (2010)

[5] J. Vrana, M. Goldammer, U. Netzelmann, “Induction and Conduction Thermography: A new Surface Inspection Method Suited for the Forging Industry”, 20th International Forgemasters Meeting, Graz, Austria (2017)

[6] K.-J. Kremer, W. Kaiser, P. Möller, “Das Therm-O-Matic-Verfahren - ein neuartiges Verfahren für die Online-Prüfung von Stahlerzeugnissen auf Oberflächenfehler”, Stahl u. Eisen 105, pp. 71-76 (1985)

[7] M. Shiratori, T. Miyoshi, T. Nakanishi, T. Noda, M. Harada, “Detection of Cracks and Measurement of Stress Intensity Factors by Infrared Video System”, JSME Int. J. I 33, pp. 400-408 (1990)

[8] G. Riegert, Th. Zweschper, G. Busse, “Lockin Thermography with Eddy Current Excitation”, QIRT Journal 1, pp. 21-32 (2004)

[9] G. Zenzinger, J. Bamberg, M. Dumm, P. Nutz, “Crack Detection using EddyTherm”, AIP Conference Proceedings 760 pp. 1646-1653 (2005)

[10] B. Oswald-Tranta, G. Wally, “Thermo-Inductive Investigations of Steel Wires for Surface Cracks”, SPIE 5782, pp. 245-254 (2005)

[11] U. Netzelmann, H. Strauß, G. Walle, “Zerstörungsfreie thermographische Methoden zur Detektion von Fehlern an Massivumform-Teilen”, Schmiede-Journal, pp. 26-28 (2007)

[12] S. Benzerrouk, R. Ludwig, “Infrared Detection of Defects in Powder-Metallic Compacts”, Journal of NDE 26, pp. 1-9 (2007)

[13] X. Maldague, and S. Marinetti, “Pulse Phase Infrared Thermography”, J. Appl. Phys. 79, pp. 2694-2698 (1996)

[14] C. Homma, “Untersuchungen zu Mechanismus und technischer Umsetzung der akustischen Thermographie”, Shaker, Herzogenrath (2009)

[15] M. Rothenfusser, C. Homma, “Acoustic Thermography: Vibrational Modes of Cracks and the Mechanism of Heat” AIP Conference Proceedings 760, pp. 624 (2005)